

Photino flux limits from the Harvard-Purdue-Wisconsin underground detector

A. Schwartz

Physics Department, Harvard University, Cambridge, Massachusetts 02138

D. Joutras and D. Cline

Physics Department, University of California, Los Angeles, California 90024

(Received 2 October 1987)

We calculate the cross section for photino-electron scattering, and use it to calculate how many photino interactions will occur in 1 kiloton of water. We then use data from the HPW (Harvard-Purdue-Wisconsin) water Čerenkov detector to determine an upper limit on the maximum allowable photino flux incident on Earth. The limit is given as a function of photino mass, initial photino energy, and selectron mass.

INTRODUCTION

In recent years much theoretical work has focused on supersymmetry,¹ a theory which accounts for the elementary scalars needed to break the $SU(2) \times U(1)$ symmetry of the standard model. Supersymmetry (SUSY) also helps stabilize the low-energy scale of electroweak symmetry breaking in the presence of other large scales in the theory (the hierarchy problem), and local SUSY theories provide a natural framework for gravitation.²

Nearly all current SUSY models incorporate a conserved multiplicative quantum number called R parity.³ Specifically,

$$R = (-1)^{3B + L + 2J}, \tag{1}$$

where B is the baryon number, L lepton number, and J spin. Since all standard-model quarks and leptons have $3B + L = 1$ and $J = \frac{1}{2}$, they carry quantum number $R = 1$. Their supersymmetric partners, however, have $J = 0$ or 1 and thus carry $R = -1$. This implies that the lightest SUSY particle (LSP) is absolutely stable, since decay to other SUSY particles is kinematically forbidden and decay to standard quarks and leptons violates R conservation.

If supersymmetric interactions and decays are taking place throughout the Universe, for example, in stellar media, then there would be a net flux of LSP's permeating space. We expect these LSP's to interact weakly due to the relatively large mass (i.e., GeV/c^2) of the exchanged SUSY propagator. The process is similar to neutrino interactions, which are weak due to heavy W or Z exchange. Since the mass range of exchange selectrons and squarks is $\sim (m_W, m_Z)$, the interaction cross section for LSP's should have the same order of magnitude as the cross section for neutrinos. Thus, various large underground detectors searching for neutrino fluxes should have roughly the same sensitivity to LSP fluxes.

In this paper we take the LSP to be the photino,⁴ the supersymmetric spin- $\frac{1}{2}$ partner of the photon, and calculate how many photino interactions are expected in a 1-kton water Čerenkov detector. We use this information to set limits on the maximum allowable photino flux us-

ing data from the Harvard-Purdue-Wisconsin (HPW) detector in Park City, Utah.

THE HPW DETECTOR

The HPW nucleon-decay detector operated from May 1983 to October 1984 and was located in Park City, Utah at a vertical depth of 1450 meters of water equivalent (mwe). Details of the experimental apparatus can be found in Refs. 5-7. The detector consisted of a cylindrical tank of 5.6 m radius and 7 m height, filled with 690 metric tons of purified water as shown in Fig. 1. Immersed in the water was a cubic lattice of 704 five-inch photomultiplier tubes set to trigger on the Čerenkov light radiated from a charged particle traversing the water medium. The custom-built phototubes had no mirror on the rear surface in order to allow for light collection over

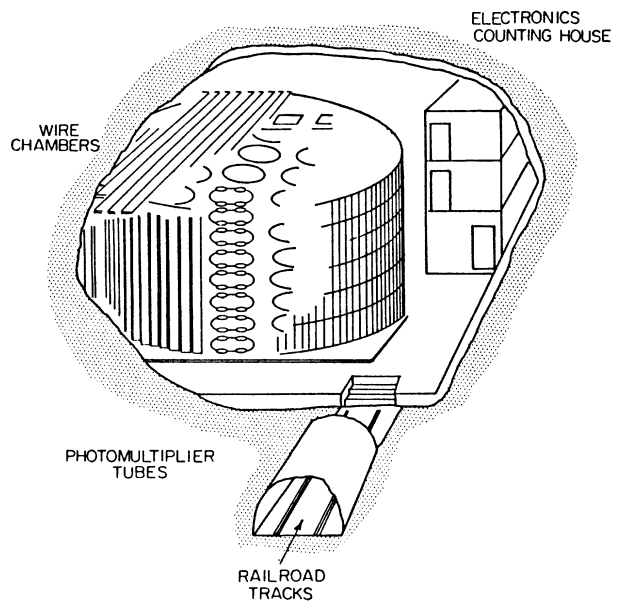


FIG. 1. Cutaway view of the HPW detector.

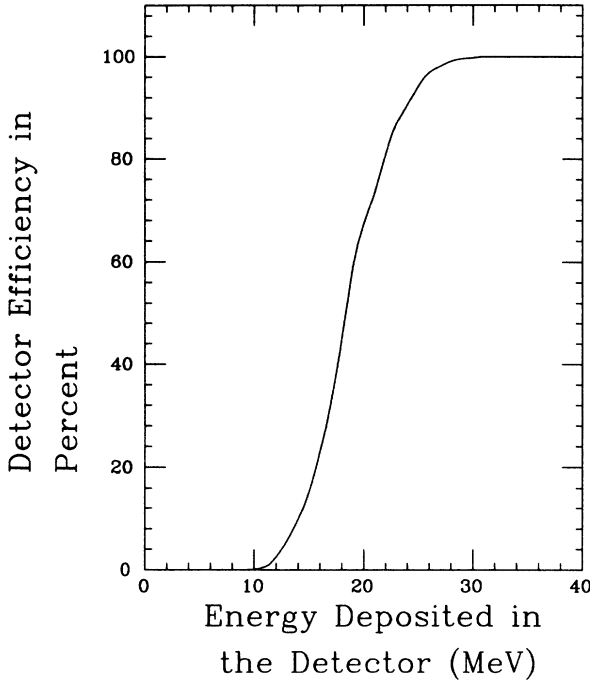


FIG. 2. Efficiency of the HPW detector as a function of the deposited energy.

$> 3\pi$ solid angle, and had a spectral sensitivity well matched to the characteristics of Čerenkov light in water.⁶

The inside walls of the tank were entirely covered with aluminized, Teflon-coated mirrors of high reflectance. These mirrors improved light collection efficiency by reflecting light that ordinarily would be absorbed by the dark tank walls. The overall uniformity of light collection was also improved. The water was constantly circulated through a filtration system, taking a total of 48 h to purify the entire volume of the detector. The final purified water had an attenuation length for Čerenkov light of about 15 m.

A limited tracking capability was provided by an array of 422 proportional wire chambers surrounding the tank, each chamber 6.1 m long and 15 cm wide. These chambers allowed us to discriminate against charged particles which originated from outside the tank, thus helping us reduce background from cosmic-ray muons.

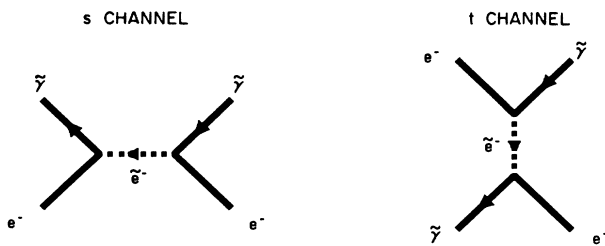


FIG. 3. *s*- and *t*-channel scattering of photinos and electrons. The arrows indicate flow of quantum number $R = -1$.

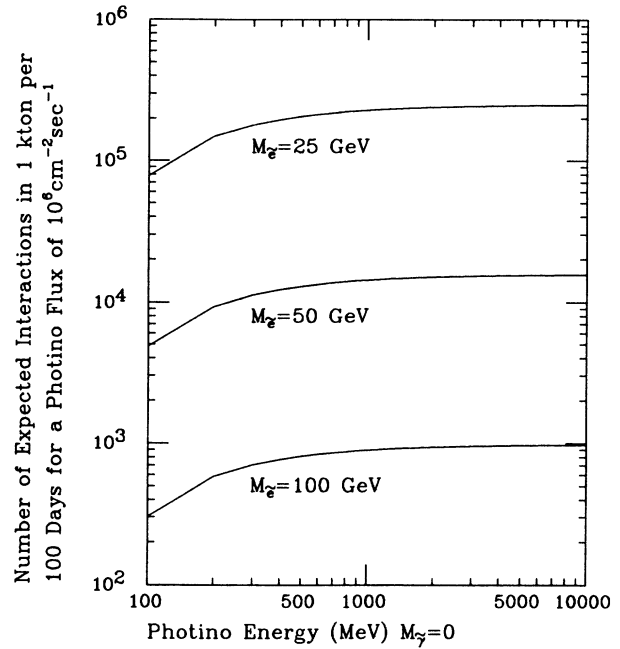


FIG. 4. Interactions per kton per 100 days for a flux of $10^6 \text{ cm}^{-2} \text{ sec}^{-1}$ massless photinos.

The trigger pulses are generated by a 50-nsec coincidence among six or more photomultiplier tubes (PMT's) located in at least three different clusters (1 cluster = 3 columns of 8 PMT's = 24 PMT's). At least 2 PMT's from each cluster must fire. Studies of muon-decay electrons from muons stopping in the tank indicate that the trigger threshold corresponds to the amount of Čerenkov light emitted by a 10-MeV electron. Figure 2 shows the efficiency of the detector as a function of the

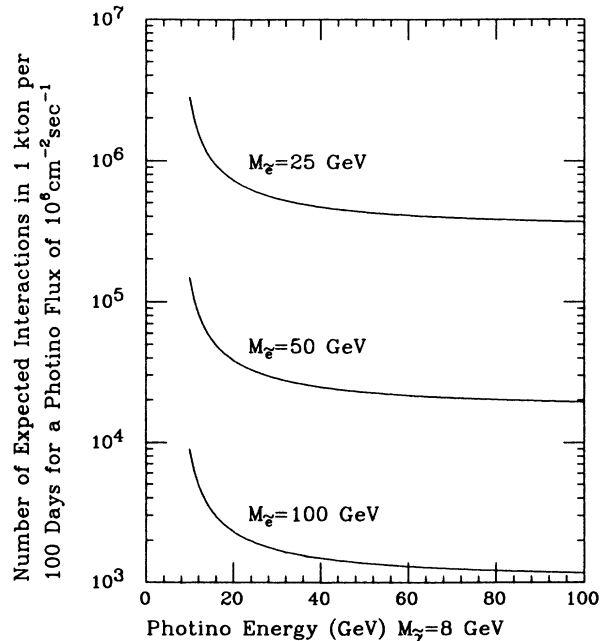


FIG. 5. Interactions per kton per 100 days for a flux of $10^6 \text{ cm}^{-2} \text{ sec}^{-1}$ photinos of $8 \text{ GeV}/c^2$ mass.

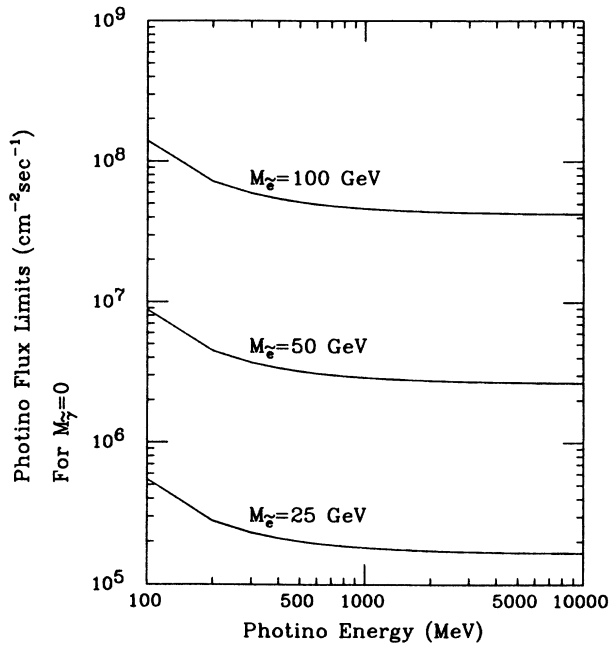


FIG. 6. Flux limits for massless, monochromatic photinos as a function of photino energy.

amount of energy deposited in it.

The trigger initiates readout of the light arrival times and intensities from each PMT, with a 2.7-nsec timing resolution for each hit. The proportional wire chambers were also read out for each event, and the point at which a charged particle passed through a wire tube was determined by charge division. The overall trigger rate was 0.63 Hz.

The PMT anode and wire-chamber pulses traveled 60

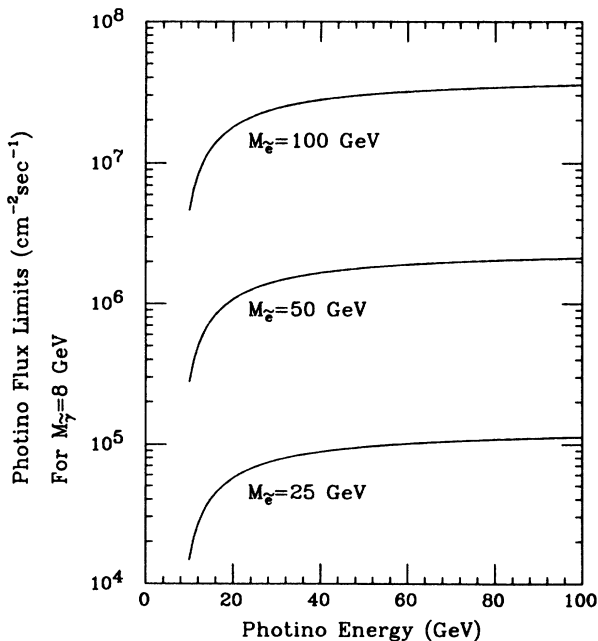


FIG. 7. Flux limits for monochromatic photinos of mass 8 GeV/c² as a function of photino energy.

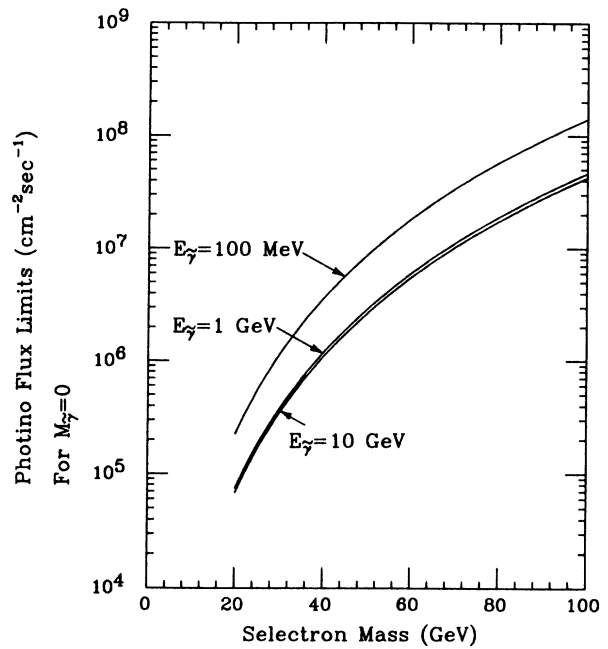


FIG. 8. Flux limits for massless, monochromatic photinos as a function of selectron mass.

m from the detector to an underground counting house. All pulse-height and time digitizers were located in this house along with a PDP-11/23 microcomputer which supervised readout and wrote data to tape.

DATA SETS

In our analysis we use data from November 1983 to October 1984 for a total of 172.5 live days. During this

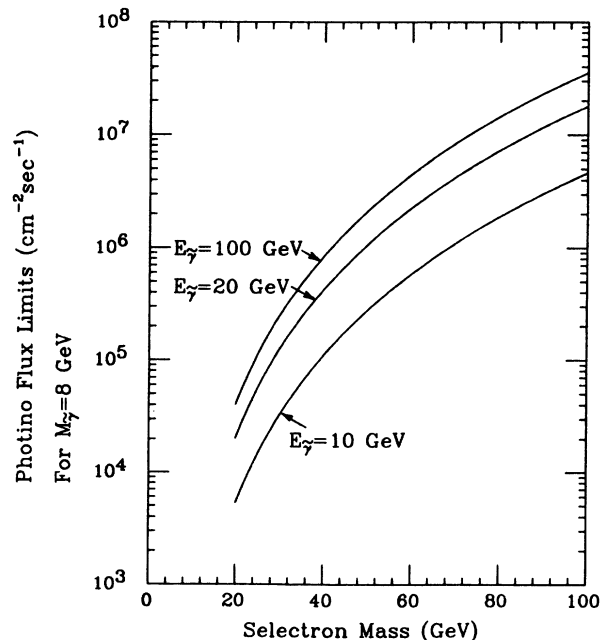


FIG. 9. Flux limits for monochromatic photinos of mass 8 GeV/c² as a function of selectron mass.

period a total of 9.4×10^6 triggers were recorded.

The rock overburden serves to filter out low-energy cosmic-ray muons and cosmic-ray-initiated electromagnetic showers, which together have a flux of $\approx 100 \text{ m}^{-2} \text{ sec}^{-1} \text{ sr}^{-1}$ at the surface. At our depth, the remaining muon flux is $\approx 0.007 \text{ m}^{-2} \text{ sec}^{-1}$. To eliminate most muon-induced events and events in which a muon is created, we require that an event has less than 51 PMT "hits." This corresponds to 75 MeV or less deposited in the tank.

We eliminate most of the PMT singles rates by noting that this background typically causes a PMT to trigger with a signal strength [ADC (analog-to-digital-converter) count] equal to or close to the PMT's pedestal value. We thus remove those hits with ADC counts closer to the pedestal value than to the value one expects from Čerenkov light in the tank. Requiring these filtered events to satisfy the trigger condition results in a sample of 5.2×10^5 events.

The sample still contains backgrounds from high-energy muons which just clip the corner of the tank and low-energy muons which decay just below the Čerenkov threshold such that only their electrons are detected. To reduce these background sources, a fiducial cut is made which halves the active volume (and hence the number of photino interactions), but reduces the number of "corner-clippers" and low-energy muon events by a factor of 10.

To eliminate the fraction of triggers remaining due to PMT singles rate and spurious electronic noise, we limit our data sample to those events with 13 or more PMT hits. This corresponds to greater than 18 MeV deposited in the tank. Finally, we reject all events which have associated wire-chamber hits, leaving a final sample of 23 551 events.

CROSS SECTIONS

To calculate flux limits, we consider the elastic-scattering process $\tilde{\gamma}e \rightarrow \tilde{\gamma}e$. The outgoing electron Čerenkov radiates in the water medium, triggering the detector. We neglect the processes $\tilde{\gamma}q \rightarrow \tilde{\gamma}q$ and $\tilde{\gamma}q \rightarrow \tilde{g}q$, which are expected to occur 3–4 orders of magnitude less frequently than the electron-scattering case.⁸ Our resultant flux limits will therefore be very slightly conservative.

The *s*- and *t*-channel Feynman diagrams are shown in Fig. 3. The two processes are distinct for fixed electron and photino helicities if the electron and photino are massless. The matrix element's interference term can thus be neglected for the case where all particles are relativistic. The differential cross section is found to be

$$\frac{d\sigma}{dy} = \frac{e^4 m_e}{2\pi p_\gamma} \left[\frac{(E_\gamma + m_\gamma)^2}{(s - m_e^2)^2} + \frac{[E_\gamma(1-y) + m_\gamma]^2}{(t - m_e^2)^2} \right], \quad (2)$$

where E_γ is the energy of the incoming photino, y is the fraction of incoming energy which is transferred to the electron, $t = (P_\gamma - P_e)^2$ and $s = (P_\gamma + P_e)^2$.

We integrate this expression over the range of y corresponding to an outgoing electron energy of 10–75 MeV. Multiplying the result by an incident flux of 10^6 photinos per cm^2 per second and scaling by the number of target electrons in a 1-kton water detector, we find the interaction rates shown in Figs. 4 and 5. Figure 4 takes photinos to be massless, while Fig. 5 takes $m_\gamma = 8 \text{ GeV}/c^2$. The rates are shown for different selectron masses, and for massless photinos reach a plateau for $E_\gamma > 1 \text{ GeV}$. For $m_e = 50 \text{ GeV}/c^2$, this plateau is $\sim 10^4$ interactions per 100 days live time.

FLUX LIMITS

In order to obtain the maximum allowable photino flux, we assume that all 23 551 photinolike events recorded which deposited between 18 and 75 MeV in the detector are due to photino interactions. The 95% upper confidence limit is that amount of flux which has a 5% chance of producing $\leq 23 551$ events after cuts. To calculate this we fold together $d\sigma(\tilde{\gamma}e \rightarrow \tilde{\gamma}e)/dE'$ and $\mathcal{C}(E')$, where E' is the outgoing electron energy and $\mathcal{C}(E')$ is the detection and selection efficiency (Fig. 2), and integrate from $E' = 18$ to 75 MeV. Multiplying this effective cross section by the number of electrons in the fiducial volume of the detector gives the number of interactions expected per unit flux. The flux is then scaled to give an expected number high enough such that there is only a 5% chance that the actual number of interactions Poisson-fluctuates below 23 551.

The calculated $d\sigma(\tilde{\gamma}e \rightarrow \tilde{\gamma}e)/dE'$ and hence the final flux limits depend on the incident photino energy E_γ and selectron and photino masses. E_γ is expected to follow some energy spectrum which can only be guessed at. In the absence of any "good guess" we take E_γ to be constant; i.e., incident photinos are monochromatic. Since energy spectra from two-body decays are monochromatic and many thermal distributions have narrow widths, this assumption can serve as a useful approximation.

Our results appear in Figs. 6–9. Figure 6 shows the flux limits as a function of E_γ for massless photinos and selectron masses of 25, 50, and 100 GeV/c^2 . Since the cross section for massless photinos increases with rising photino energy, the flux limits decrease. For $m_e = 50 \text{ GeV}/c^2$, the photino flux is $\leq 8.8 \times 10^6 \text{ cm}^{-2} \text{ sec}^{-1}$ for $E_\gamma > 100 \text{ MeV}$, and $\leq 2.7 \times 10^6 \text{ cm}^{-2} \text{ sec}^{-1}$ for $E_\gamma > 1 \text{ GeV}$. In contrast, the cross section for massive photinos decreases with rising photino energy, causing flux limits to become more conservative. This is shown in Fig. 7, in which m_γ is taken to be 8 GeV/c^2 . As E_γ becomes larger and m_γ becomes negligible, the cross sections and flux limits of Fig. 7 converge to those of Fig. 6. The lim-

its become approximately independent of incident photino energy for $E_\gamma > 40$ GeV.

Similarly, Figs. 8 and 9 show photino flux limits as a function of selectron mass for $m_{\tilde{\gamma}} = 0$ and $8 \text{ GeV}/c^2$, respectively. In both cases the flux limits become more conservative as $m_{\tilde{e}}$ increases, since a heavier propagator decreases the cross section. The limits increase by 3 orders of magnitude as $m_{\tilde{e}}$ increases from 20 to 100 GeV/c^2 . Both plots converge to the same values as E_γ becomes large.

ACKNOWLEDGMENTS

We gratefully acknowledge the efforts of the following members of the Harvard-Purdue-Wisconsin Collaboration, without whom this experiment would not have been possible: E. Aprile, K. L. Giboni, T. J. Phillips, C. Rubbia, D. Winn, and W. Worstell from Harvard; J. Gaidos, R. McHenry, J. Negret, T. Palfrey, G. Sembrowski, and C. Wilson from Purdue; and G. Kalkanis, R. Loveless, R. March, J. Matthews, A. More, and R. Morse from Wisconsin.

¹See, for example, H. E. Haber and G. L. Kane, Phys. Rep. **117**, 75 (1985); S. Dawson, E. Eichten, and C. Quigg, Phys. Rev. D **31**, 1581 (1985).

²J. Wess and J. Bagger, *Supersymmetry and Supergravity* (Princeton University Press, Princeton, NJ, 1983).

³P. Fayet, Phys. Lett. **69B**, 489 (1977); G. Farrar and P. Fayet, *ibid.* **76B**, 575 (1978).

⁴See, for example, M. Drees, C. S. Kim, and X. Tata, Phys. Rev. D **37**, 784 (1988).

⁵D. B. Cline, *ICOBAN '83*, proceedings of the International Colloquium on Baryon Nonconservation, Frascati, Italy,

1983, edited by E. Bellotti and S. Stipcich (Servizio Documentazione de Laboratori Nazionali di Frascati dell'INFN, Frascati, 1983).

⁶B. Worstell, Ph.D. thesis, Harvard University, 1986.

⁷T. Phillips, Ph.D. thesis, Harvard University, 1986; J. M. Matthews, Ph.D. thesis, University of Wisconsin—Madison, 1984; D. Joutras, Ph.D. thesis, University of Wisconsin—Madison, 1987.

⁸S. Midorikawa and S. Yoshimoto, Phys. Lett. B **171**, 239 (1986).

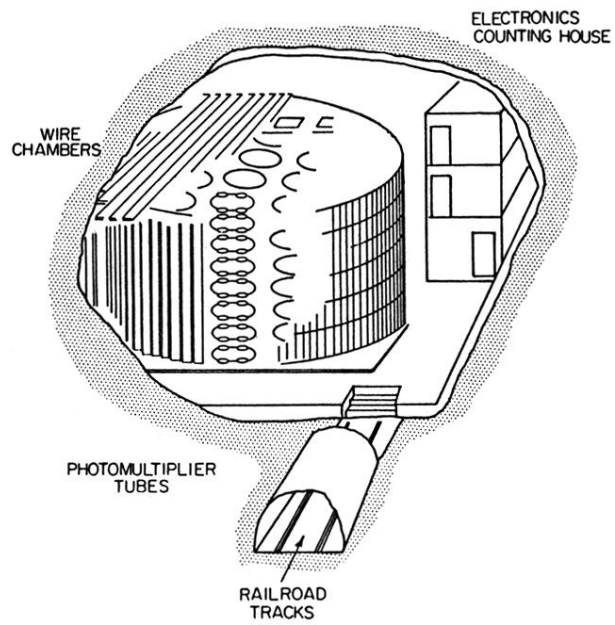


FIG. 1. Cutaway view of the HPW detector.